A THEORETICAL MODEL WITH VARIABLE MASSES FOR THE MOLTEN FUEL-SODIUM THERMAL INTERACTION IN A NUCLEAR FAST REACTOR

L. CALDAROLA*

Institut für Angewandte Systemtechnik und Reaktorphysik, Kernforschungszentrum Karlsruhe, D-75 Karlsruhe, Germany

SUMMARY

In the model proposed in this paper, the reaction has been assumed to occur in two successive phases, which have been called respectively phase A and phase B.

Phase A. A given number (function of time) of fuel particles comes in intimate contact with a given mass of liquid sodium (function of time). The heat transfer process is characterized by very good direct thermal contact between the fuel and the liquid coolant, and by a large contact area due to the small size of the particles. The heat transfer coefficient decreases with time due to the formation of a temperature profile inside the fuel particles. The heated volume of sodium is constrained by the surrounding unheated coolant and by the other materials present in the core. The mechanical constraint is schematized by a sodium column of finite length which is contained in a channel located above the reaction volume. The sudden expansion of the heated volume first produces acoustic waves which travel along the sodium column. Later the sodium column behaves like a piston which is pushed inertially upwards. The pressure rises, reaches a maximum, and then falls as soon as the expansion of the liquid sodium becomes important. At the time at which the pressure reaches the saturation point, sodium boiling starts and phase B begins.

Phase B. The heat transfer process is now characterized by a very large contact area, and by a thermal contact between the fuel and the coolant which becomes increasingly worse with time, due to the formation of a sodium vapour layer at the external surface of the fuel fragments. The sodium will boil in a large quantity, and will produce therefore large volume changes. The sodium piston will be further accelerated and its movement will allow the pressure in the reaction volume to decrease.

The model accounts for the time history of the temperatures of each fuel particle by means of the use of specially averaged temperature values. The calculation of the heat transfer coefficient during phase B is based on experimental results. The presence of fission gases can also be taken into account. A size distribution of fuel particles has also been incorporated in the model as well as the effect of the friction due to the channel walls and that of the pressure losses at the outlet of the channel. Numerical evaluations are also included and the results are discussed. It has been concluded that the total work produced strongly decreases with the time constant of the vapour film layer around the particles and increases with the speed with which the fuel breaks down in fragments and mixes with the liquid sodium. The effect of the length of the sodium column has also been investigated.

---

* (Euratom delegate to the Fast Reactor Project.)

1. Introduction

The mixing of hot molten fuel with liquid coolant in a sodium-cooled fast reactor has long been recognized /Ref. 1/ as a potential hazard, in that it may lead to violent coolant vaporization. The events producing the mixing may arise from different causes, such as an accidental power transient followed by fuel meltdown and rupture of the cladding, or a partial (or complete) interruption of the normal sodium flow followed by sodium boiling, channel voiding, fuel melting, and finally sodium re-entry into the channel.

Experimental research programs /Ref. 2/ have been started in various countries with the purpose of investigating fuel coolant interaction (FCI) in order to understand its mechanism, to measure its violence, as well as to evaluate consequences on the surrounding structures. Experiments have been carried out in which various reactor conditions were simulated. However, due to the multiplicity of the phenomena which occurr, the interpretation of these experiments is very difficult.

Since the interpretation of the experiments does not yet seem to provide enough information which can be used by engineers /Ref. 2/, and since on the other side sodium cooled fast reactors must be built in the meanwhile, a second approach is being followed in parallel to the experimental program. This approach consists in assuming that a large FCI can occur and in evaluating its consequences. Parametric models have been developed in various countries /Ref. 2/ with the scope of analyzing the FCI in order to reduce the degree of conservatism imposed by early methods. The central problem seems to be the evaluation of the heat flux rate (as a function of the time) from the fuel to the coolant and the diffusion of the heat into the surrounding sodium.

The heat flux rate is proportional to the product of the contact area available for the heat flow and the heat transfer coefficient between the fuel and the coolant. The contact area between fuel and coolant depends upon the degree of the fuel dispersion inside the coolant, while the heat transfer coefficient is effected by the physical state of the coolant at the boundary surface between the fuel particles and the coolant, and by the temperature profile inside the fuel particles.

The contact area is strongly influenced by the way in which the molten fuel is released from the failed fuel element, and by the fuel fragmentation and mixing with sodium which take place during the interaction.

As long as fuel release, fragmentation and mixing with sodium will be not well understood, it will be not possible to develop a model which describes these phenomena exactly. "Post fragmentation analysis" after FCI allows us to measure the size distribution of the small fuel fragments.

A theoretical model describing a FCI in a reactor channel has been developed by the author /Ref. 3 and 4/ which is characterized by constant masses of fuel and coolant participating in the interaction and by fuel fragments being spheres all having the same radius. Succesively variable masses both for fuel and sodium have been invorporated in the model and in addition a log-normal distribution has been assumed for the radii of the fuel particles. This model has been partially described already in Ref. 5 and 7 and it has been fully described in this paper.

2. Preliminaries

The FCI is assumed to take place in two successive phases.

Phase A

A given number (function of time) of fuel particles come in intimate contact with a given mass of liquid sodium (function of time). The heat transfer process is characterized by very good direct thermal contact between the fuel and the liquid coolant, and by a large contact area due to the small size of the particles. The thermal resistance for the heat flow from the fuel to the coolant increases with time due to the formation of a temperature profile inside the fuel particles.

The heated volume of sodium is constrained by the surrounding unheated coolant and by the other materials present in the core. The mechanical constraint is in our model schematized by a sodium column (Fig. 1) of finite length contained in a channel and located above the reaction volume. The sudden expansion of the heated volume first produces acoustic waves which travel along the sodium column. Later the sodium column behaves like a piston which is pushed inertially upwards.

The pressure rises, reaches a maximum, and then falls as soon as the expansion of the liquid sodium becomes important. At the time at which the pressure reaches the saturation point, sodium boiling starts and phase B begins.

Phase B

The heat transfer process is now characterized by a very large contact area, and by a thermal contact between the fuel and the coolant which becomes increasingly worse with time, due to the formation of a sodium vapour layer at the external surface of the fuel fragments. The sodium will boil in a large quantity, and will produce therefore large volume changes. The sodium piston will be further accelerated and its movement will allow the pressure in the reaction volume to decrease.

The heat transfer process during both phases has been assumed to occur isentropically, which means also that no heat gets out from the reaction volume into the surrounding space. The thermal conductivity of the liquid sodium participating in the interaction has been assumed to be infinite. The time history of the temperature of each fuel particle has been taken into account, and the exact solution of the heat conduction equation in a sphere has also been included in the model. Volume changes due to the fuel are assumed to be negligible. Fission gases, when present, are assumed to be perfect gases. In addition it is assumed that they don't insulate thermically the fuel particles and that they are compressed isentropically. The effect of the size distribution of the fuel particles has been taken into account for phase A only.

3. Equations governing phase A

During phase A the sodium remains liquid. A very good direct thermal contact is assumed to take place between the fuel particles and the liquid sodium. Phase A is characterized by the following equations (see list of symbols).

Equation of the Sodium temperature

$$\Theta = \Theta_o + \frac{c_f}{c_{eff}} \frac{\int_o^t M_f \left[T_o - \Theta\right] h \left(\frac{t-t'}{t_f};\sigma\right) dt'}{\bar{t}_f \, M_c} \qquad (1)$$

Equation of the pressure

$$\frac{dP}{dt} = A\left[\frac{d\Theta}{dt} - \frac{S\rho_\ell}{\alpha M_c}\frac{d\eta}{dt} + \frac{\rho_\ell}{\alpha M_c^2}\frac{dM_c}{dt}(S\eta + B) - C\right] \qquad (2)$$

where

$$c_{eff} = \bar{c}_{\ell sat} + \frac{1}{\Theta-\Theta_o}\left[K - K_o - \frac{1}{M_c}\int_o^t \frac{M_c}{\rho_\ell}\frac{dP}{dt'}\,dt'\right] \qquad (3)$$

$$\rho_\ell = \rho_{\ell sat}\exp\left[\int_{P_{sat}}^{P} \alpha dP'\right] \qquad (4)$$

with $\rho_{\ell sat}$; α and P_{sat} calculated at the temperature "Θ".

$$\bar{t}_f = \frac{\rho_f c_f \bar{R}_f^2}{\lambda_f} = \text{time scale of average fuel particle} \qquad (5)$$

$$K = \int_{P_{sat}}^{P} \frac{1-\alpha\gamma\Theta}{\rho_\ell}\,dP' \qquad (6)$$

$$K_o = \int_{P_{sato}}^{P_o} \frac{1-\alpha\gamma\Theta_o}{\rho_\ell}\,dP' \qquad (7)$$

with the integration carried out along the isothermals "Θ" (Eq. 6) and Θ_o (Eq. 7).

$$A = \frac{1}{1 + \frac{\phi}{n}\frac{M_f}{M_c}\frac{\rho_\ell}{\rho_f}\frac{1}{\alpha P}(P_o/P)^{1/n}} \qquad (8)$$

$$B = \phi\frac{M_f}{\rho_f}\left[1 - (P_o/P)^{1/n}\right] \qquad (9)$$

$$C = \frac{\phi}{\alpha M_c}\frac{\rho_\ell}{\rho_f}\left[1 - (P_o/P)^{1/n}\right]\frac{dM_f}{dt} \qquad (10)$$

The equations of the mechanical constraint are given in section 5. The equation of the physical parameters of Sodium α; γ; $\rho_{\ell sat}$; P_{sat} are given in Appendix. The characteristic function of the first type "$h(t/\bar{t}_f;\sigma)$" describing the heat conduction in a sphere has been obtained in Ref. 3 and 10.

Fig. A1-1 shows the function $h(t/\bar{t}_f;\sigma)$ for two different values of "σ".

Eq. 1 has been obtained in Ref. 10 by properly combining the energy balance equation between fuel and sodium and the equations of heat transfer from each fuel particle to the liquid sodium.

Eq. 2 is the equation of the conservation of volume and it has been obtained in Ref. 10.

4. Equations governing phase B

Fuel particles are assumed to remain all together within the liquid sodium in a portion of the reaction volume (schematic diagram of Fig. 2) while the sodium vapour (mixed vapour) flows away and pushes the sodium piston upwards. The sodium vapour surrounding the fuel particles (vapour film) is only a very small percentage of the total vapour.

Fig. 3 shows a spherical fuel particle enveloped in a vapour bubble. The particle releases heat to the surrounding coolant. The liquid evaporates at the portion of the coolant surface nearest to the fuel fragment, and the vapour flows away along the space between the fuel surface and the liquid surface generating a force which tends to push the fuel particle away from the liquid. Heat is transferred from the fuel particle to the liquid sodium by conduction and radiation through the moving vapour film between the lower half of the particle and the boundary surface. Mass is removed from the liquid by evaporation into the vapour film on the lower surface. A pressure gradient in the vapour film causes it to flow and the integrated product of the pressure (above the bubble pressure) and the horizontal projection of the lower half of the particle supports the particle.

The conservative hypothesis has been made that the upper half of the fuel particle will also produce vapour by assuming the lower liquid boundary surface to be ideally extended above the upper half of the particle (Fig. 3). The vapour produced by the upper half of the particle is assumed of course not to contribute to the support of the particle. The model of Fig. 3 was already described in Ref. 3.

Phase B is characterized by the following equations (see list of symbols).

Energy equation

$$c_f \frac{d\left[M_f(T_o-\bar{T})\right]}{dt} = \left[\bar{c}_{\ell sat}(\Theta-\Theta_o) - K_o\right]\frac{dM_c}{dt} + L\frac{d(xM_c)}{dt} +$$

$$+ M_c\frac{d\Theta}{dt}\left[c_{\ell sat} + x\frac{dL}{d\Theta} - \frac{dP}{d\Theta}\left(\frac{1-x}{\rho_\ell} + \frac{x}{\rho_v}\right)\right] \qquad (1)$$

Equation of the heat leaving the fuel

$$c_f M_f \frac{\bar{T}_w-\Theta}{\tau_b}\,\frac{1+y_{eff}}{y_{eff}} = c_f\frac{d\left[M_f(T_o-\bar{T})\right]}{dt} \qquad (2)$$

Equation of the heat conduction in the fuel

$$\bar{T}_w = T_o - \int_0^t \frac{1}{M_f}\,\frac{d\left[M_f(T_o-\bar{T})\right]}{dt}\,k\left(\frac{t-t'}{\bar{t}_f}\right)dt' \qquad (3)$$

Equation of the effective thickness of the vapour layer

$$\frac{dy_{eff}}{dt} = \frac{1}{3(1+y_{eff})^2}\left\{\frac{\rho_f}{\rho_v}\,\frac{1}{M_f}\,\frac{d(xM_c)}{dt} - \frac{\rho_f g\bar{R}_f\,y_{eff}^3}{1.5\mu}\left[1+\frac{\bar{c}_b(\bar{\Theta}_b-\Theta)}{L}\right] -\right.$$

$$\left. -\left(3y_{eff}+3y_{eff}^2+y_{eff}^3\right)\frac{1}{M_f}\,\frac{dM_f}{dt}\right\} \qquad (4)$$

Equation of the conservation of the volume

$$xM_c = \frac{\rho_v}{\rho_\ell - \rho_v}\left[M_c\left(\frac{\rho_\ell}{\rho_o} - 1\right) + \rho_\ell(Sn + B)\right] \tag{5}$$

where

$$\bar{\Theta}_b = \frac{1}{2}\left[(1 - D)\,\bar{T}_w + (1 + D)\,\Theta\right] \tag{6}$$

$$D = \frac{y_{eff} \cdot (2 + y_{eff})}{y_{eff}^2 + 3y_{eff} + 3} \tag{7}$$

$$\tau_b = \frac{\rho_f c_f \bar{R}_f^2}{3\lambda_b} = \text{film time constant} \tag{8}$$

The equations of the mechanical constraint are given in section 5.

The equations of the physical parameters of sodium are given in Appendix. The characteristic function of the second type $k(t/\bar{t}_f)$ describing the heat conduction in a sphere has been obtained Ref. 10. The function $k(t/\bar{t}_f)$ is shown in Fig. A1-2.

Eqs. 1 to 5 have been obtained in Ref. 10. The equations 6-8 were already obtained in Ref. 3.

The main simplificative hypothesis used in phase B are the following.

1. Sodium vapour has been assumed to be in thermal equilibrium with its liquid. This means that the "mixed vapour" (Fig. 2) is saturated vapour and has the same temperature of the liquid. Calculations carried out in Ref. 4 show that this assumption produces neglibible errors in the results.
2. Since the vapour around the fuel particles is only a small percentage of the total vapour, the enthalpy of the vapour in Eq. 1 has been assumed to be the same as that of the "mixed vapour". The density of the vapour film has also been assumed to be equal to that of the "mixed vapour".
3. The time history of the temperatures of each fuel particle has been taken into account by means of the use of some effective values: $\bar{T}$; $\bar{T}_w$ and y_{eff} (see Ref. 10). Another model in which the fuel particles have been classified into groups characterized by the time at which they come in contact with the liquid sodium has been developed in Ref. 8.

Before closing this section the authour likes to point out three arguments which show that the model for phase B can be considered conservative, which means that with this model heat transfer rates are calculated, which probably exceed those of reality.

(1) The upper part of the fragment has been assumed (as far as the heat transfer is concerned) to be effective as much as the lower part which is nearer to the liquid (Fig. 3).

(2) The second hypothesis is that the fuel particles are assumed to remain all together with the liquid sodium in a portion of the reaction room (Fig. 2) while the sodium vapour (mixed vapour in Fig. 2) flows away and pushes the sodium piston upwards. The sodium vapour

surrounding the fuel particles (vapour film in Fig. 2) is only a very small percentage of the total vapour which is produced. In reality the fuel particles will be mixed together with the sodium vapour and will be distributed all around the reaction volume (rari nantes ingurgite vasto). They will be presumably entirely surrounded by sodium vapour, and therefore the heat transfer coefficient will be much lower than that calculated with this model.

(3) The third hypothesis is that the thermal conductivity of the liquid sodium has been assumed to be infinite. This is a conservative hypothesis also because the phase B initiates when the sodium bulk temperature reaches the saturation temperature, which happens surely at a time later than that at which the sodium temperature at the boundary with the fuel particles reaches the saturation temperature.

The proposed model is of course conservative only within the constraint of the assumption that a vapour film grows around the fuel particles. Since the experimental results of Ref. 6 seem to confirm this hypothesis, the author concludes that the proposed model for phase B should provide a more realistic and sufficiently conservative description of the phenomena which occur when the sodium vaporization does take place.

5. The equations of the mechanical constraint

We have the following equations

Acoustic approximation $(t < t_{ac} = \frac{2\ell_o}{c_o})$

$$\frac{d\eta}{dt} = \frac{P - P_o}{\rho_o c_o} \tag{1}$$

Inertial approximation $(t > t_{ac})$

$$\frac{d^2\eta}{dt^2} = \frac{P - P_\ell}{\rho_o(\ell_o - \eta)} - g - \frac{\varepsilon}{\ell_o}\left(\frac{d\eta}{dt}\right)^2 \tag{2}$$

where

$$P_\ell = P_{ext} + \frac{1}{2} h_s \rho_o \left(\frac{d\eta}{dt}\right)^2 \tag{3}$$

and

$$\varepsilon = \frac{\text{Friction factor x channel perimeter x piston initial length}}{\text{channel cross section}}$$

The validity of both approximations has been discussed in Ref. 3.

6. Numerical evaluations

Calculations have been carried out with the objective to investigate the effect of some important parameters. The following parameters have been kept the same in all the cases, which have been calculated.

P_{ext} = 2 atm
T_o = 2900 ^oK
Θ_o = 1100 ^oK
R_f = 117 μ
$\varepsilon = h_s = 0$

For the fuel thermal conductivity "λ_f" the very pessimistic value of 0.05 Watt/cm^{O}K has been assumed.

The masses of the fuel and sodium participating in the interaction are assumed to be both linear functions of the time

$$M_f = \begin{cases} M_{f\infty} \cdot \dfrac{t}{\tau_f} & \text{for } t < \tau \\ M_{f\infty} & \text{for } t \geq \tau_f \end{cases}$$

and

$$M_c = \begin{cases} M_{c\infty} \dfrac{t}{\tau_c} & \text{for } t < \tau_c \\ M_{c\infty} & \text{for } t \geq \tau_c \end{cases}$$

with

$$\frac{M_{f\infty}}{M_{c\infty}} = 8.3 \text{ in all cases}$$

The length "L_m" of the mixing zone

$$L_m = \frac{M_{c\infty}}{S\rho_o}$$

has been put equal to 17.5 cm in all cases. All calculations have been carried out up to the point in which the channel is empty, because beyond this point the sodium expands almost without contraint and the additional work produced is therefore negligible.

In all the cases it has been put $M_{c\infty}$ = 1 gr.

6.1 The effect of the fragmentation time constant "τ_f"

In this set of calculations the mass of sodium has been assumed to be constant (τ_c = 0, that is istantaneous mixing). In addition the initial length "ℓ_o" of the sodium column above the reaction volume has been assumed to be 120 cm and the film time constant "τ_b" has been put equal to 0.31 secs, which corresponds to the value of $6.5 \cdot 10^{-4}$ Watt/cm$\cdot^O$K of the thermal conductivity of the sodium vapour. Table 1 shows the peak pressure as a function of τ_f. The peak pressure decreases with "τ_f", as one should expect. Table 2 shows the work of phase A, that of phase B and the total work as functions of τ_f. The total work decreases rapidly with "τ_f" up to 10 msecs (1st region). Afterwards it decreases slowly up to 20 msec (2nd region) and then rapidly again (3rd region). The explanation for this behaviour is the following. The rapid reduction in the first region is due to the fact that the work during phase A decreases rapidly with τ_f. In the second region the work decreases slowly, because the contribution of phase A has already become a small percentage of the total work. The contribution of phase B increases first and then decreases (but not rapidly) in the first region and increases slowly in the second region. This is due to the fact that during the phase B the slowing down of the fragmentation and mixing process has essentially the effect of only delaying the pressure pulse (Fig 4).

In the third region of Table 2, the work decreases rapidly with "τ_f", because "τ_f" is larger than the time needed to empty the channel (see Table 3). This means that at the time at which the channel is empty only a fraction of the total mass of fuel "$M_{f\infty}$" has participated in the interaction.

6.2 The effect of the mixing time constant "τ_c"

Tables 1 and 4 show respectively the peak pressure and the total work as functions of "τ_c" in the cases $\tau_c = \tau_f$ and $\tau_c = 0$. The values of the case $\tau_c = \tau_f$ are lower than the corresponding values of the case $\tau_c = 0$. The difference however reaches only 20 % for $\tau_f = 50$ msec. Fig. 5 shows the pressure transient in the three following cases

1st Case: Fuel to coolant mass ratio increasing with time
($\tau_f = 10$ msecs.; $\tau_c = 0$)

2nd Case: Fuel to coolant mass ratio constant with time
($\tau_f = \tau_c = 10$ msecs.)

3rd Case: Fuel to coolant mass ratio decreasing with time
($\tau_f = 0.5$ msecs; $\tau_c = 10$ msecs.)

The three pressure transients are different. Differences in the total work between the two extreme cases is about 10 % (Table 5). It is interesting to notice that the duration of Phase A in the first case is as short as $5 \cdot 10^{-4}$ msecs.

6.3 The effect of the film time constant "τ_b"

Fig. 6 shows the pressure transient in the following three cases (in all cases $\tau_f = 10$ msecs. and $\tau_c = 0$)

Case 1 $\tau_b = 0.031$ secs.
Case 2 $\tau_b = 0.31$ secs.
Case 3 $\tau_b = 3.1$ secs.

Table 6 gives the values of the total work done as a function of "τ_b". One can conclude that "τ_b" has a very strong effect, and that large values of "τ_b" enormously reduce the pressure and the total work done (this last by a factor of about 10). This is due to the fact that for large values of "τ_b" the fuel particles are practically thermically isolated during phase B, so that the expansion of the sodium takes place almost adiabatically. In Fig. 7 the fuel and sodium temperatures as functions of the time are shown for the two cases $\tau_b = 0.031$ and 3.1 secs. It is important to point out that vapour blanketing is very effective only if it is associated with a fragmentation (and/or mixing) time constant. The reason for this is the following: in the case of very rapid fragmentation and mixing, the sodium has already received most of its heat at the end of phase A. Vapour blanketing during phase B is therefore not very effective. This can be seen from the curves of Fig. 8 (pressure as a function of time). For the curves Nr. 1 (istantaneous fragmentation and mixing) the difference between the fuel temperature "$\bar{T}$" and the sodium temperature "Θ" at the end of phase A was only of 180 ^{o}K, while for the curves Nr. 2 ($\tau_f = 10$ msecs., $\tau_c = 0$) "$\bar{T} - \Theta$" was equal to 650 ^{o}K. The total work is shown in Table 7. The results of Table 7 confirm that the total work is sensitive to "τ_b" only if the fragmentation (and/or mixing) process is not rapid.

6.4 The effect of the initial length "ℓ_o" of the sodium piston

Calculation have been carried out with a larger initial length of the sodium piston ($\ell_o = 460$ cm). The results are shown in Table 8 where they are compared to the corresponding results of the case $\ell_o = 120$ cm. The results show that in the case of $\ell_o = 460$ cm the total work does not decrease so stronghly with "τ_f" as in the case $\ell_o = 120$ cm. A reduction can be obtained by increasing "τ_b". In fact in the case ℓ_o = 460 cm τ_f = 10 msecs and τ_b = 0.31 secs, the work is 206 Joule. If now τ_b is increased to 3.1 secs the work decreases to 123 Joule. Fig. 9 shows the pressure as a function of the time in the case τ_f = 10 msecs and ℓ_o = 120 and 460 cm.

6.5 The effect of fuel particles size distribution and of gas content

Calculations have been carried out to account for the fuel particles size distribution (σ = 1.36) and for fission gases (ϕ = 0.2). The results are shown in Figs. 10 and 11, from which it appears that the effects of size distribution and of gas content are important only for very rapid fragmentation and mixing.

7. Conclusions

The main conclusions are the following

1. Total work stronghly decreases with the fragmentation and/or mixing time constants. For values of τ_f (or τ_c) larger than 5 msecs further reduction is not very important.
2. Vapour blanketing during phase B is effective only if it is accompained by a relatively slow process of fragmentation and mixing.
3. It is possible to considerably reduce the total work, if one uses higher values of the film time constant "τ_b". The value of 0.31 secs for "τ_b" is based on an average value of the thermal conductivity of the saturated sodium vapour. The vapour around the particles is yet superheated, so that its thermal conductivity is expected to be lower than that of the saturated vapour. This should procude a larger value of "τ_b", which in turn reduces the total work.
4. The total work rises with the initial length of the sodium piston. This confirms the importance of a good simulation of the mechanical constraint.
5. The effects of fuel particles size distribution and gas content are important only for rapid fragmentation and mixing.

In order to further reduce the degree of the conservativism in this theoretical model, future work will follow the following lines.

1. To get information about the thermal conductivity of superheated sodium vapour.
2. To include in the model the effect of heat loss from the reaction volume. This should particularly reduce the total work in the case of very long sodium pistons.
3. To use a more sophisticated model for the mechanical constraint. This can be obtained by using the american REXCO code to simulate the mechanical constraint in two dimensions (Ref. 9).

Work must be continued also on the present model to investigate the friction effect due to the channel walls ($\varepsilon \neq 0$) and that due to the concentrated pressure losses at the channel outlet ($h_s \neq 0$).

8. Acknowledgements

The author wishes to thank Mr. Wickenhäuser (IASR) for having carried out the necessary calculations on the IBM 370/168 Computer.

9. List of symbols

Θ = coolant (sodium) temperature

Θ_o = initial coolant temperature

c_f = fuel specific thermal capacity

c_{eff} = coolant effective specific thermal capacity

M_f = mass of fuel participating in the interaction

$h(t/\bar{t}_f;\sigma)$ = characteristic function describing the heat transfer process in a sphere (1st type)

t = time

t_f = time scale of a fuel particle

$\bar{t}_f$ = time scale of average fuel particle

σ = mean deviation of the lg-normal distribution of the fuel particles radii

M_c = mass of ccolant participating in the interaction

P = pressure in the interaction zone

γ = thermal pressure coefficient of the liquid coolant

S = channel cross section

ρ_ℓ = density of the liquid coolant

$\rho_{\ell sat}$ = density of the saturated liquid (coolant)

α = isothermal compressibility of the liquid coolant

η = increase of the height of the interaction zone due to the expansion of coolant and gas

ρ_o = initial density of coolant

L_m = length of the mixing zone

ρ_f = fuel density

λ_f = fuel thermal conductivity

ϕ = initial gas to fuel volume ratio

n = exponent of the isentropic compression of the gases = 1.4

P_o = initial pressure in the interaction zone

$\bar{T}_w$ = average surface temperature of the fuel particles

y_{eff} = effective ratio between the vapour film thickness and the particles radius

τ_b = vapour film time constant

$\bar{c}_{\ell sat}$ = liquid specific heat capacity at the coolant along the saturation line averaged between θ_o and θ

$c_{\ell sat}$ = liquid specific heat capacity of the coolant along the saturation line

L = coolant vaporization heat

x = mass percentage of coolant vapour

ρ_v = vapour density (ccolant). In this paper it has been put $\rho_v = \rho_{vsat}$

ρ_{vsat} = density of the saturated vapour (coolant)

T_o = initial fuel temperature

$\bar{T}$ = average fuel temperature

$k(t/\bar{t}_f)$ = characteristic function describing the heat transfer process in a sphere (2nd type)

P_{sat} = saturation pressure of the coolant

P_{sato} = $\left[P_{sat} \right]_{\theta = \theta_o}$

g = gravity acceleration = 980 cm/sec^2

t_{ac} = acoustic time

μ = dynamic viscosity of the vapour (coolant)

$\bar{c}_b$ = vapour specific heat capacity at constant pressure averaged between θ_o and θ

$\bar{\theta}_b$ = average temperature of vapour films

λ_b = thermal conductivity of vapour films

ℓ_o = initial length of sodium piston

P_{ext} = external pressure

τ_f = fragmentation time constant

τ_c = mixing time constant

$M_{f\infty}$ = total fuel mass participating in the interaction

$M_{c\infty}$ = total coolant mass participating in the interaction

$\bar{R}_f$ = average particles radius

c_o = sound velocity in the liquid coolant

P_{ext} = pressure at the channel outlet

h_s = coefficient of concentrated pressure losses at channel outlet

ε = coefficient of pressure losses due to the channel walls

References

[1] HICKS and MENZIES, "Theoretical studies on the fast reactor maximum accident", ANL 7120, 1965

[2] CALDAROLA, "Current status of knowledge of molten fuel/sodium thermal interaction", Paper presented at a meeting of the european "safety working group", February 26/27th 1974, and KFK 1974

[3] CALDAROLA, "A theoretical model for the molten fuel-sodium interaction in a nuclear fast reactor", Nucl. Eng. and Design, Vol. 22, No. 2, October 1972, pages 175-211

[4] CALDAROLA, KOUTSOUVELIS, "Theoretical models for the molten fuel-sodium interaction", International Conference on Engineering of Fast Reactors for Safe and Reliable Operation, Karlsruhe, October 1972

[5] CALDAROLA, KOUTSOUVELIS, "The Karlsruhe variable mass model for the description of the fuel/coolant interaction", O.E.C.D. Second Specialist Meeting on "Sodium fuel interaction in fast reactors", Ispra, Nov. 1973

[6] HALL et al., "Inverse Leidenfrost Phenomenon", Nature 224 (1969)

[7] CALDAROLA, KOUTSOUVELIS, "A theoretical model with variable masses for molten fuel-sodium interactions" Conference on fast reactor safety, Beverly Hills, California, April 1974

[8] KOUTSOUVELIS, "Ein theoretisches Modell zur thermischen Brennstoff-Natrium-Wechselwirkung mit variablen Massen und mehreren Gruppen von Brennstoffpartikeln" (in preparation)

[9] CHANG, GVILDIS, FISTEDIS, "Two dimensional hydrodynamics analysis for primary containment", ANL 7498 (Nov. 1969)

[10] CALDAROLA, "A theoretical model with variable masses for the molten fuel-sodium thermal interaction in a nuclear fast reactor (topical report) KFK 2078 (in preparation)

Appendix

Physical properties of fuel and sodium

A. Fuel

c_f = 0.5023 Joule/gr. ^oK

ρ_f = 8.76 gr./cm^3

λ_f = 0.05 Watt/cm ^oK

The effect of the latent heat of fusion "H_f" can be taken into account by increasing the initial fuel temperature "T_o" by the amount "ΔT" given by

$$\Delta T = \frac{H_f}{c_f} = \frac{275}{0.5023} = 549\ ^oK$$

B. Sodium (from Ref. 1)

$$\alpha = 2.96\cdot10^{-5}+5.56\cdot10^{-8}(\theta-1160)+0.89\cdot10^{-5}\exp\left[-(\theta-1000)/267\right]\ \left[atm^{-1}\right] \text{ for } \theta > 1000^oK$$

$$\gamma = \frac{dP_{sat}}{d} - \frac{d\rho_{\ell sat}}{d\theta}\frac{1}{\alpha\ \rho_{\ell sat}}\quad [atm/^oK]$$

$$P_{sat} = \theta^{-0.61344}\exp\left(15.3838 - \frac{1.27677\cdot10^4}{\theta}\right)\ [atm]$$

$$\rho_{\ell sat} = 0.95413-1.2735\cdot10^{-4}\left(\frac{9}{5}\theta - 460\right)-4.60037\cdot10^{-9}\left(\frac{9}{5}\theta-460\right)^2 + \\ +9.667\cdot10^{-13}\left(\frac{9}{5}\theta - 460\right)^3\quad [gr/cm^3]$$

$$c_{\ell sat} = 4.186(1.9434-2.103\cdot10^{-3}\theta+6.7254\cdot10^{-7}\theta^2)\ \left[\frac{Joule}{gr.\ ^oK}\right]$$

$$c_{\ell sat} = 4.186\left[1.9434-1051\cdot10^{-3}(\theta+\theta_o) + 2.2418\cdot10^{-7}(\theta^2+\theta\theta_o+\theta_o^2)\right]\left[\frac{Joule}{gr.\ ^oK}\right]$$

$$L = 4.831\cdot10^3\left(\frac{2780-\theta}{2780}\right)^{0.4092}\quad\left[\frac{Joule}{gr.}\right]$$

$$\rho_{vsat} = \frac{P_{sat}}{\theta R Z_{sat}}$$

R = gas constant for 1 gr. of sodium = 3.565 cm$^3\cdot$atm/gr. ^oK

Z_{sat} = compressibility factor = $-0.97258 + 0.42417\cdot10^{-2}\,\theta - 0.28996\cdot10^{-5}\,\theta^2 + 0.55424\cdot10^{-9}\,\theta^3$

$\bar{c}_b = 2.3\ \frac{Joule}{gr.\ ^oK}$

$\lambda_b = 6.5\cdot10^{-4}\ \frac{Watt}{cm\ ^oK}$

$\mu = 2.6\cdot10^{-4}\ \frac{dyne\ sec}{cm^2}$

Table 1

Peak pressure as a function of the fragmentation (τ_f) and mixing (τ_c) time constants (ℓ_o = 120 cm; τ_b = 0.31 secs.)

τ_f (msecs)	Peak pressure (atm)	
	$\tau_c = 0$	$\tau_c = \tau_f$
0	5555	5555
1	1931	1342
2	1243	763
5	647	331
10	336	173
20	157	56
50	60	36
100	36	28

Table 2

Works as functions of the fragmentation time constant "τ_f"
(τ_c = 0; $_o$ = 120 cm τ_b = 0.31 secs)

	τ_f (msecs)	Work (Joule)		
		Phase A	Phase B	Total
	0	325	56	381
	1	121	62	183
1st Region	2	59	54	113
	5	15	45	60
	10	3.7	46.3	51
	20	0.8	51	50
2nd Region	50	0.1	42	42
3rd Region	100	< 0.1	28.5	28.5

E 1/1*

Table 3

Time "T_e" to empty the reactor channel as a function of the fragmentation (τ_f) and mixing (τ_c) time constants (ℓ_o = 120 cm; τ_b = 0.31 secs)

τ_f (msecs)	T_e (msecs)	
	$\tau_c = 0$	$\tau_c = \tau_f$
0	4.8	4.8
1	6.1	6.8
2	7.9	9.7
5	12.5	15.4
10	18.0	19.3
20	25.0	24.3
50	36.4	28.7
100	48.2	32.3

Table 4

Total work as a function of the fragmentation (τ_f) and of the mixing (τ_c) time constants (ℓ_o = 120 cm; τ_b = 0.31 secs)

τ_f (msecs)	Work (Joule)	
	$\tau_c = 0$	$\tau_c = \tau_f$
0	381	381
1	183	143
2	113	79
5	60	52
10	51	49
20	50	43
50	42	30
100	28.5	23

Table 5

E 1/1*

Total work as a function of the fragmentation (τ_f) and mixing (τ_c) time constants (ℓ_0 = 120 cm; τ_b = 0.31 secs)

τ_f (msecs)	τ_c (msecs)	Work (Joule)
0.5	10	46
10	10	49
10	0	51

Table 6

Total work as a function of the vapour film time constant "τ_b"
(τ_f = 10 msecs; τ_c = 0 ℓ_0 = 120 cm)

τ_b (secs.)	Work (Joule)
$3.1 \cdot 10^{-4}$	106
$3.1 \cdot 10^{-3}$	103
$3.1 \cdot 10^{-2}$	92
⊠ $3.1 \cdot 10^{-1}$	51
3.1	16.5
$3.1 \cdot 10$	10
$3.1 \cdot 10^{2}$	9.8

⊠ Value of τ_b based on an average value of the thermal conductivity of the saturated sodium vapour ($6.5 \cdot 10^{-4}$ Watt/cm °k)

E I/1*

Table 7

Total work as a function of the vapour film (τ_b) and fragmentation (τ_f) time constants. (τ_c = 0 ℓ_o = 120 cm)

τ_b (secs.)	τ_f (msecs)	Work (Joule)
$3.1 \cdot 10^{-3}$	0	408
$3.1 \cdot 10^{-1}$	0	381
$3.1 \cdot 10^{-3}$	10	103
$3.1 \cdot 10^{-1}$	10	51

Table 8

Total work as a function of the fragmentation time constant "τ_f" and of the initial length "ℓ_o" of the sodium piston.
(τ_c = 0; τ_b = 0.31 secs.)

τ_f (msecs)	Work (Joule)	
	ℓ_o = 120 cm	ℓ_o = 460 cm
0	381	495
1	183	307
2	113	262
5	60	225
10	51	206 ⊠
20	50	191
50	42	187

⊠ In the case τ_b = 3.1 secs, the total work would be reduced to 123 Joule.

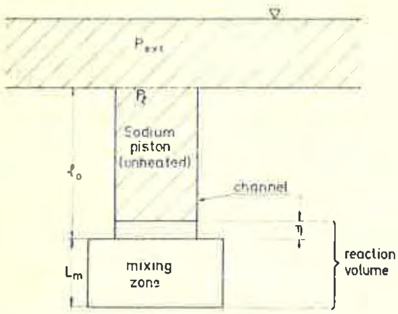

Fig.1 Schematic diagram of the "one dimension mechanical constraint"

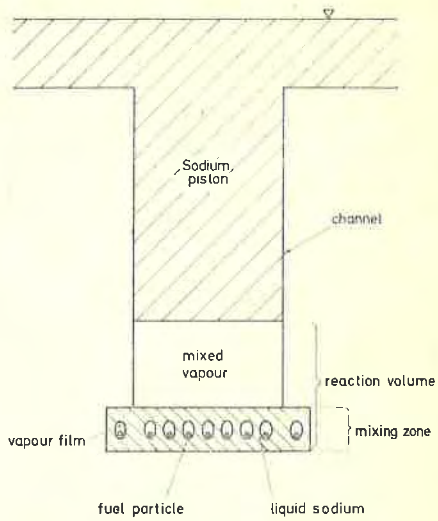

Fig. 2 Schematic diagram showing the location of the fuel particles, of the liquid sodium and of sodium vapour inside the reaction volume

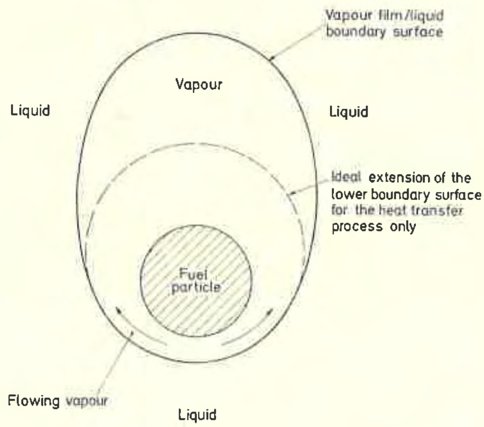

Fig. 3 Schematic Diagram of the Heat Transfer Process from a Fuel Particle to the Liquid Sodium During Phase B

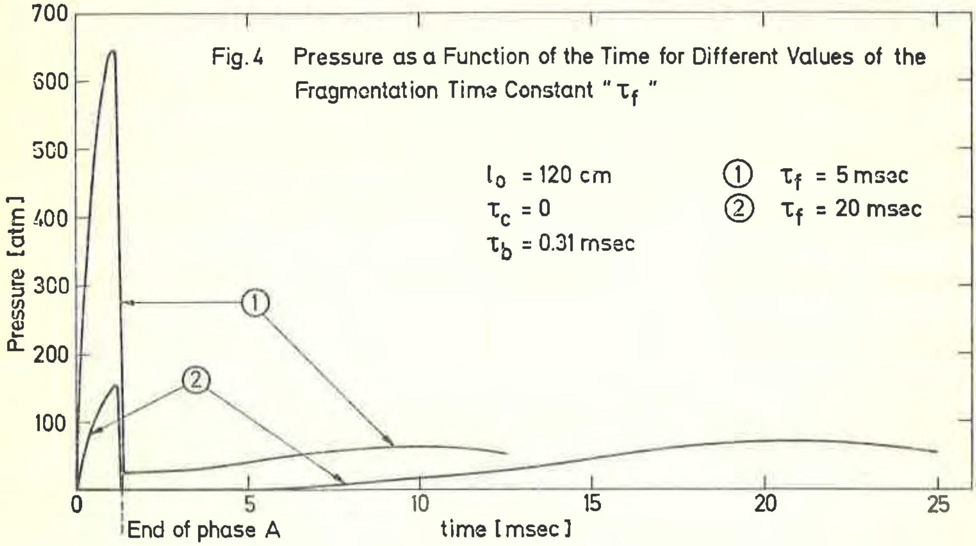

Fig. 4 Pressure as a Function of the Time for Different Values of the Fragmentation Time Constant "τ_f"

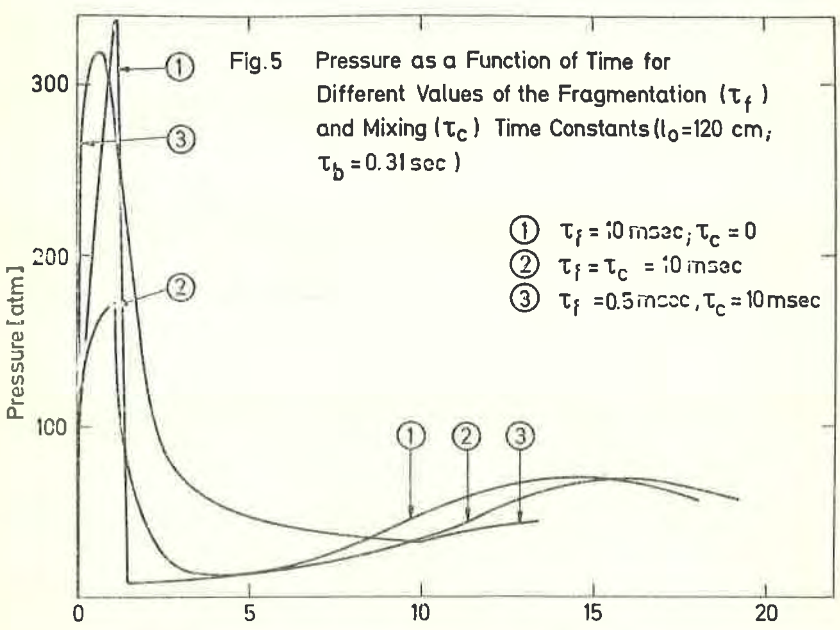

Fig. 5 Pressure as a Function of Time for Different Values of the Fragmentation (τ_f) and Mixing (τ_c) Time Constants (l_0=120 cm; τ_b = 0.31 sec)

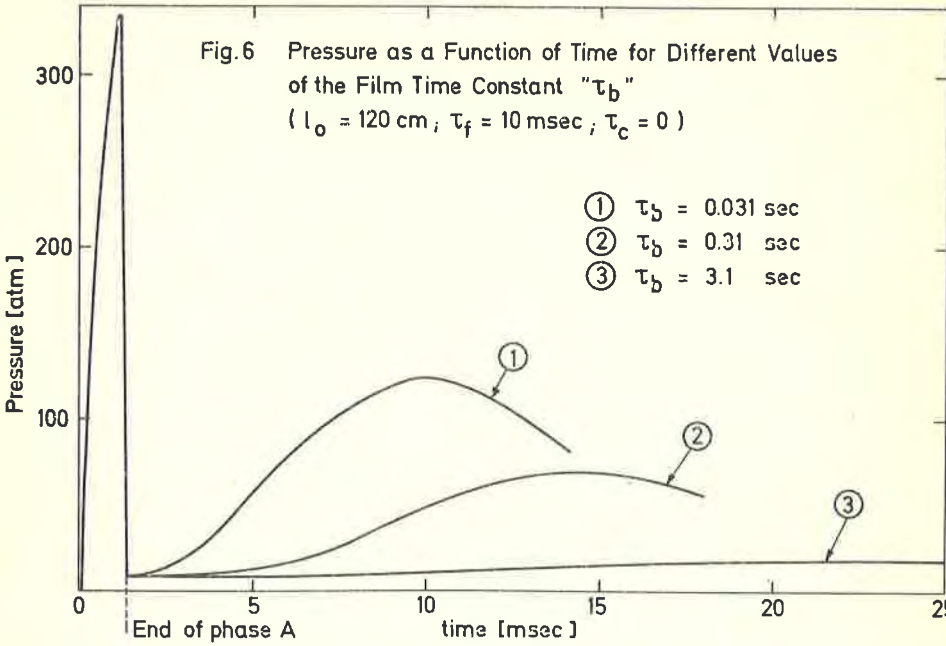

Fig. 6 Pressure as a Function of Time for Different Values of the Film Time Constant "τ_b"
(l_o = 120 cm ; τ_f = 10 msec ; τ_c = 0)

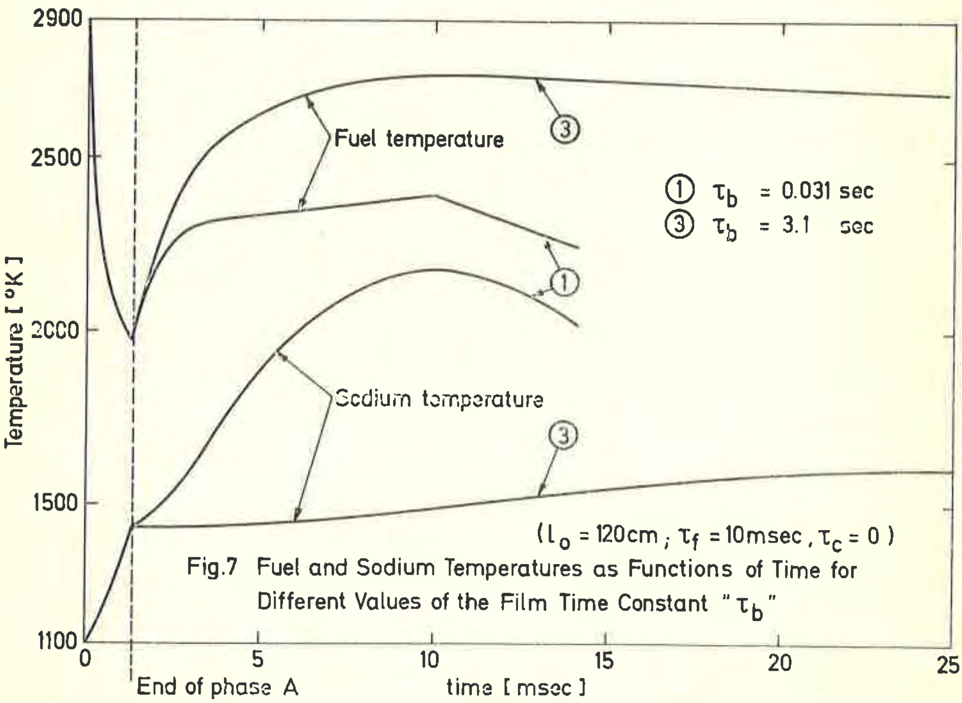

(l_o = 120cm ; τ_f = 10msec , τ_c = 0)
Fig. 7 Fuel and Sodium Temperatures as Functions of Time for Different Values of the Film Time Constant "τ_b"

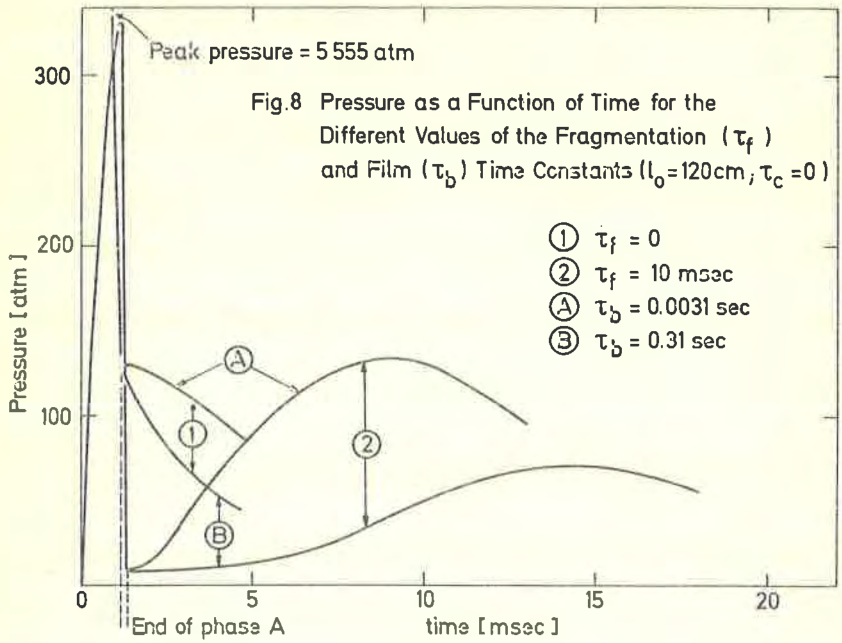
Peak pressure = 5 555 atm
Fig.8 Pressure as a Function of Time for the Different Values of the Fragmentation (τ_f) and Film (τ_b) Time Constants (l_o = 120 cm ; τ_c = 0)
① τ_f = 0
② τ_f = 10 msec
Ⓐ τ_b = 0.0031 sec
Ⓑ τ_b = 0.31 sec
Pressure [atm]
300
200
100
0
5
10
15
20
End of phase A
time [msec]

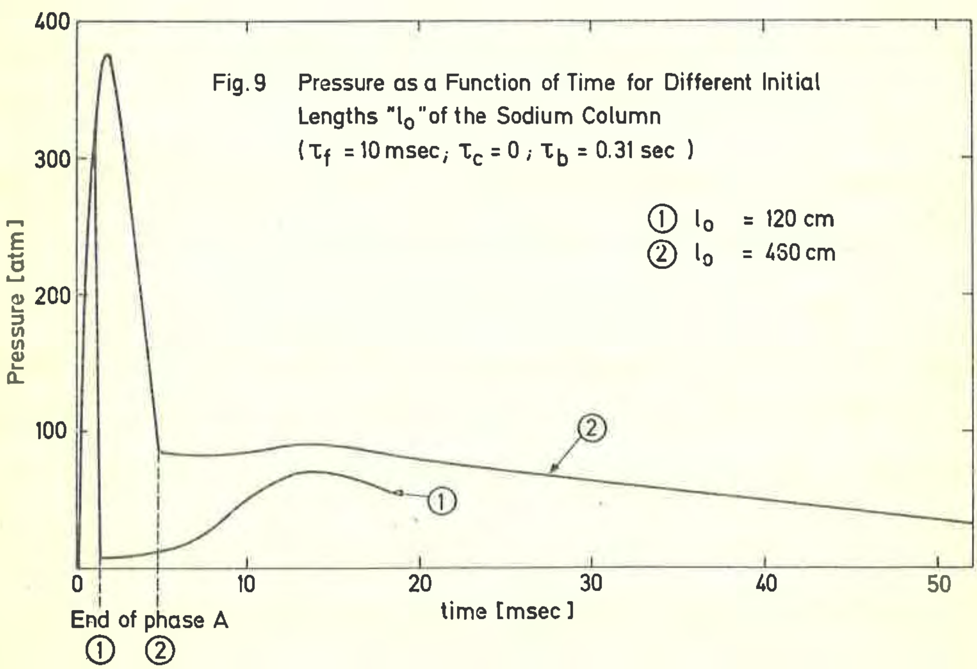
Fig. 9 Pressure as a Function of Time for Different Initial Lengths "l_o" of the Sodium Column (τ_f = 10 msec ; τ_c = 0 ; τ_b = 0.31 sec)
① l_o = 120 cm
② l_o = 460 cm
Pressure [atm]
400
300
200
100
0
10
20
30
40
50
time [msec]
End of phase A
① ②

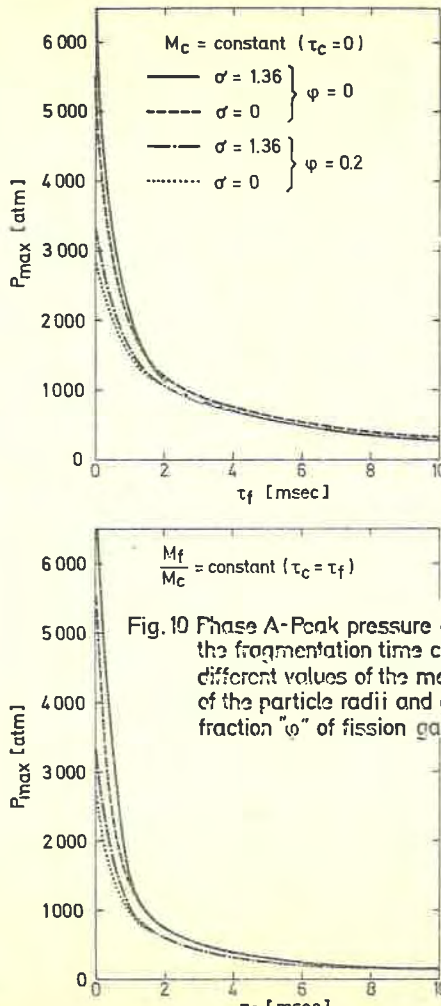

Fig. 10 Phase A-Peak pressure as a function of the fragmentation time constant "τ_f" for different values of the mean deviation "σ" of the particle radii and of the volume fraction "φ" of fission gases

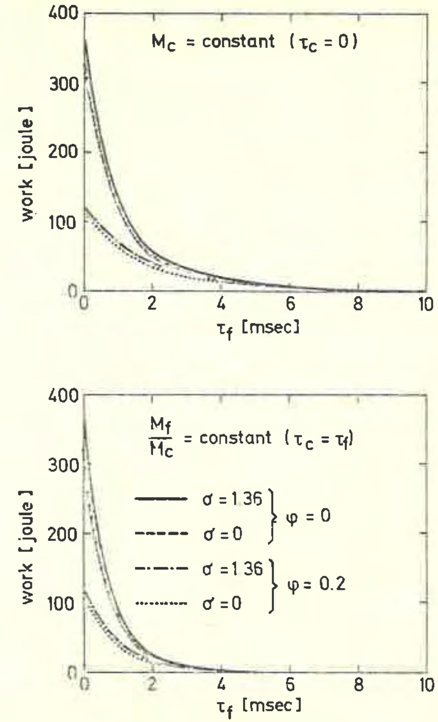

Fig.11 Phase A- Work as a function of the fragmentation time constant "τ_f" for different values of the mean deviation "σ" of the particle radii and of the volume fraction "φ" of fission gases

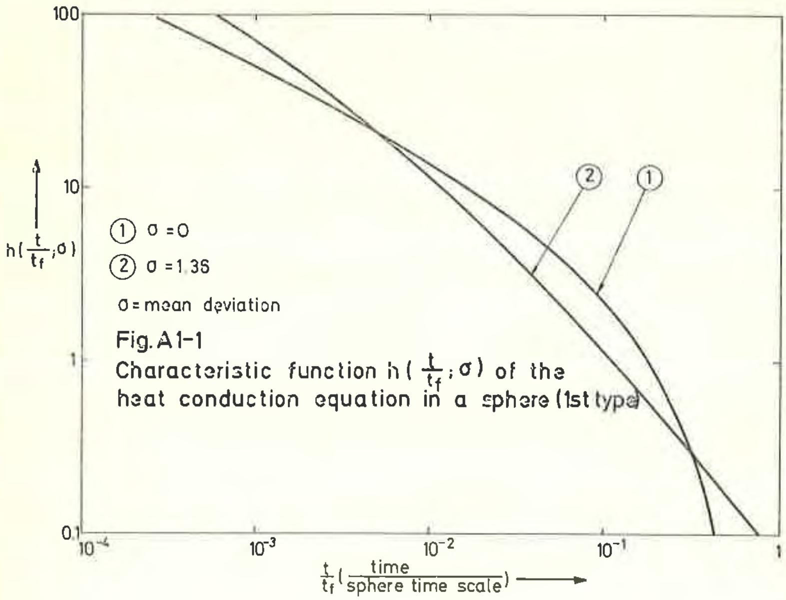

Fig. A1-1
Characteristic function $h(\frac{t}{t_f};\sigma)$ of the heat conduction equation in a sphere (1st type)

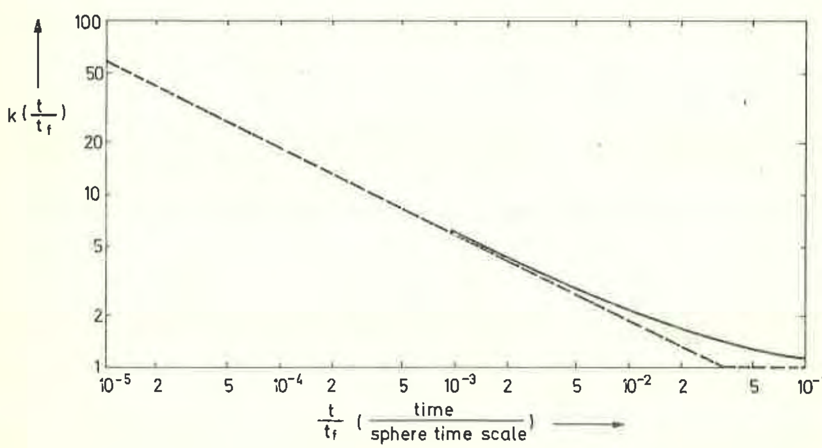

Fig. A1-2 Characteristic function "$k(\frac{t}{t_f})$" of the heat conduction equation in a sphere (2^{nd} type)